Atmospheric Research 342 (2026) 109112

Contents lists available at ScienceDirect

Atmospheric Research

journal homepage: www.elsevier.com/locate/atmosres

Size-resolved atmospheric ice-nucleating particles in a typical city located in a semi-arid region of Northwestern China

Jiayun Li [a], Dantong Chen [a], Yiyang Gao [a], Zhijun Wu [b], Jiawei Yang [b], Pengfei Tian [a,c], Yuan Wang [c], Zirui Liu [d], Lei Zhang [a,c], Zhongwei Huang [a,c,*]

[a] Key Laboratory for Semi-Arid Climate Change of the Ministry of Education, College of Atmospheric Sciences, Lanzhou University, Lanzhou 730000, China
[b] State Key Joint Laboratory of Environmental Simulation and Pollution Control, College of Environmental Sciences and Engineering, Peking University, Beijing, China
[c] Collaborative Innovation Center for Western Ecological Safety, Lanzhou University, Lanzhou 730000, China
[d] State Key Laboratory of Atmospheric Boundary Layer Physics and Atmospheric Chemistry (LAPC), Institute of Atmospheric Physics, Chinese Academy of Sciences, Beijing 100029, China

ARTICLE INFO

Keywords:
Ice-nucleating particles (INPs)
Dust
Chemical compositions
Anthropogenic pollution

ABSTRACT

Semi-arid regions are characterized by water scarcity and high sensitivity to climate change. However, there is a severe lack of observational research on ice-nucleating particles (INPs) in these areas, leading to a limited scientific understanding of the concentration, sources, and activity of INPs. Here, we report the INP number concentration, surface active-site density (n_s), and chemical compositions (water-soluble ions and metal elements) of urban particles in different size classes in Lanzhou, a typical city located in a semi-arid region. The results indicate that the particulate pollution in Lanzhou exhibited characteristics of a mixture of dust and anthropogenic pollutants, even during clean periods. The measured concentration of immersion-mode INPs increased with decreasing temperature, ranging from 0.05 to 19.60 L^{-1} between −25 °C and −10 °C. At three representative temperatures (−10, −15, and − 20 °C), the average concentrations were 0.05 ± 0.04 L^{-1}, 0.49 ± 0.43 L^{-1}, and 19.60 ± 5.78 L^{-1}, respectively. Due to the persistent presence of dust particles in the background atmosphere of Lanzhou, INP concentrations are moderately elevated compared to regions dominated by anthropogenic pollution. Chemical composition analysis reveals a notably high proportion of calcium ions and a low proportion of secondary inorganic ions. This characteristic indicates that calcium ions mainly originate from the limited dissolution of calcium carbonate, during dust transport to relatively dry semi-arid regions, low relative humidity inhibits the aqueous-phase chemical reactions between gaseous pollutants and dust surfaces (e.g., calcium carbonate), thereby impeding the formation of secondary products such as calcium nitrate and ammonium nitrate. The relationship between chemical composition and INP concentration reveals that certain metal ions (calcium and magnesium ions) exhibit a strong correlation with INPs in supermicron particles, while secondary inorganic ions show no significant correlation with INPs. This suggests that the ice-nucleating ability of particles in Lanzhou is likely dominated by transported dust, while the contribution of anthropogenic pollution may be limited. Finally, we propose a new parameterization scheme for INP activity that is based on size-resolved nucleation properties (n_s) and is applicable to mixed conditions of dust and anthropogenic pollution.

1. Introduction

Ice nucleus particles (INPs) refer to particles that initiate the deposition of water vapor or the freezing of supercooled liquid droplets to form ice crystals in the atmosphere (You, 1976). The ice-nucleating activity of INPs is highly temperature-dependent, with different types of particles becoming active at varying temperatures, typically ranging from 0 °C down to approximately −38 °C, below which homogeneous freezing dominates (Hawker et al., 2021). Through their involvement in the heterogeneous activation process of ice crystals, INPs influence the microphysical processes, lifetime, and precipitation processes of clouds, thereby indirectly affecting the Earth system's radiation balance, energy budget, global water cycle, and climate change (DeMott et al., 2010; Vergara-Temprado et al., 2018; Zhao et al., 2019). As a vital component

* Corresponding author at: Key Laboratory for Semi-Arid Climate Change of the Ministry of Education, College of Atmospheric Sciences, Lanzhou University, Lanzhou 730000, China.
E-mail address: huangzhongwei@lzu.edu.cn (Z. Huang).

https://doi.org/10.1016/j.atmosres.2026.109112
Received 12 February 2026; Received in revised form 11 May 2026; Accepted 24 May 2026
Available online 26 May 2026

of the global arid and semi-arid climate zones, the semi-arid region of Northwest China serves as a sensitive zone to global climate change. Issues such as water scarcity, ecological vulnerability, and desertification caused by aridification have severely impacted and constrained the region's economic and social development. Precipitation, as one of the key processes supplying water to semi-arid areas, holds particular importance for regions like the semi-arid Northwest China, which faces water scarcity and high sensitivity to climate change. Given the critical role of INPs in ice crystal formation and subsequent precipitation development, understanding INP characteristics in this water-scarce region is essential for improving our knowledge of local cloud and precipitation processes.

The formation of ice crystals in clouds is a critical process for precipitation development in mixed-phase and ice clouds, particularly over continental regions where precipitation is primarily generated through ice-phase processes (Mülmenstädt et al., 2015). The climate forcing of mixed-phase clouds and their resultant precipitation are highly sensitive to ice nucleus concentration, with this sensitivity exhibiting significant regional variations within mixed-phase clouds (Fan et al., 2017; Gibbons et al., 2018). Assumptions regarding mixed-phase clouds and their radiative properties represent one of the largest sources of uncertainty in climate models (Tan et al., 2016). In summary, INPs play an indispensable role in the aerosol-cloud-climate system. The semi-arid regions suffer from water scarcity and are highly sensitive to climate change. However, current scientific understanding of the ice-nucleating ability of atmospheric particles remains relatively limited, which greatly constrains research in areas such as the development and utilization of cloud water resources and the assessment of climatic effects in semi-arid regions.

The Taklamakan Desert and the Gobi Desert are significant sources of Asian dust aerosols. The emission of dust in Asia is substantial, contributing approximately 40% to the global total. Dust particles exhibit high ice-nucleating activity (Hoose and Möhler, 2012) and serve as a crucial global source of INPs, accounting for about 15–27% of ice nuclei in mixed-phase clouds worldwide (Kawai et al., 2021). Dust events can facilitate the long-range transport of bioaerosols across the globe, leading to more severe and far-reaching impacts on global climate change, human health, and ecological systems (Maki et al., 2019). In earlier years, scholars conducted observational studies on INPs in semi-arid regions, including Yinchuan in Ningxia, Bayanhot in Inner Mongolia (Niu et al., 2000), Dongsheng in Inner Mongolia (Chen, 1994), and Changji in Xinjiang (Li and Du, 2003). These studies revealed regional differences in INP concentrations and their susceptibility to meteorological conditions.

Dust aerosols are the primary aerosol type in the semi-arid regions of northwestern China. Lanzhou, a typical city located in the semi-arid regions, lies along the transport pathways of dust from the Taklamakan and Gobi deserts, with frequent dust events occurring in winter and spring. With socio-economic development and the combined influence of natural dust and anthropogenic pollution, the proportion of mixed dust and anthropogenic aerosols has steadily increased in northwestern China over the past decade (Mehta et al., 2018). Dust contributions to $PM_{2.5}$ in Lanzhou consistently exceed 20% throughout the year (Wang et al., 2016). In the 1980s, researchers utilized Bigg-type ice nucleus counters to observe INPs in Lanzhou. The average INP concentration during the observation period was 1.5 times higher than that recorded in the early 1960s in the same area, suggesting that factors such as urban development and increased atmospheric pollution may have contributed to the rise in INPs (Ge and Zhou, 1986). To sum up, Lanzhou is jointly influenced by dust aerosols and anthropogenic pollutants, leading to increasingly complex sources of INPs. However, the scarcity of observational studies severely limits the scientific understanding of ice nucleus concentrations, sources, and activities in this typical semi-arid city near the dust source regions.

In this study, size-resolved ambient particles were collected in the urban atmosphere in Lanzhou from May to October 2025. We quantified the INP concentration, surface active-site density, and chemical compositions (water-soluble ions and metal elements) of urban particles in different size classes in Lanzhou. Meanwhile, total suspended particulate (TSP) samples were collected and subjected to metagenomic sequencing to characterize the microbial community composition and functional potential associated with INPs. A new parameterization scheme for INP activity, based on size-resolved nucleation properties (n_s) and is applicable to mixed conditions of dust and anthropogenic pollution.

2. Materials and methods

2.1. Sample collection and particle number measurement

Size-resolved aerosol samples were collected on the rooftop of a building (approximately 20 m above ground level) at Lanzhou University (36.05°N, 103.87°E). Aerosols were sampled using a Micro-Orifice Uniform Deposit Impactor (MOUDI; MSP Corporation, USA) with a flow rate of 30 L min^{-1}. Particles were sampled onto 47 mm polycarbonate Nuclepore filters (0.2 μm; Whatman). The MOUDI separates particles according to their aerodynamic diameter (AD), and all particle sizes reported in this study refer to the 50% cut-off AD (D_{50}), defined as the diameter at which particle collection efficiency reaches 50%. The impactor stages used in this study corresponded to D_{50} values of 0.32, 1.0, 1.8, 3.2, and 5.6 μm. In total, seven sets of MOUDI samples were collected with sampling durations of 12 h and 24 h during both pollution and clean days in 2025. Detailed sampling information is provided in Table 1. The MOUDI size-segregation principle is based on stage-specific collection efficiency curves, as described in Marple et al. (1991), where each stage is characterized by a 50% cut-off diameter (D_{50}). The study demonstrated the existence of interstage losses and noted that particle bounce may occur under certain operating conditions, indicating that imperfect particle collection is an inherent feature of cascade impactors. Although particle bounce was not explicitly quantified or corrected, it is a recognized physical limitation of MOUDI. It may influence collection efficiency and size classification. As is reported in Chen et al. (2021), the bounce is unavoidable due to the limitation of substrates and solid particles. However, the losses rapidly decreased as the particles size decreased, and the collection efficiency curves of each stage are sharp, indicating that MOUDI is still a high-accuracy cascade impactor for collecting size-resolved particle samples.

Particle number size distributions for particles exceeding 560 nm were measured by an aerodynamic particle sizer (APS, TSI Inc., USA) during the sampling period. Both the APS and MOUDI determine particle size based on aerodynamic diameter. Particle surface area size

Table 1
Overview of the 7 sets of samples collected in 2025.*

Sample ID	Date	Starting time	$PM_{2.5}$ day average ($\mu g \cdot m^{-3}$)	PM_{10} day average ($\mu g \cdot m^{-3}$)	Classification
P1	7 May 2025	9:00	54 ± 14	146 ± 41	Polluted
P2	16 May 2025	20:00	104 ± 42	277 ± 119	Pollution affected by dust
P3	20 May 2025	20:00	32 ± 7	78 ± 13	Polluted
P4	4 Sep 2025	22:00	27 ± 12	75 ± 52	Polluted
P5	15 Sep 2025	16:00	69 ± 42	207 ± 144	Pollution affected by dust
C1	22 Sep 2025	20:00	17 ± 7	37 ± 13	Clean
C2	16 Oct 2025	16:00	21 ± 6	41 ± 20	Clean

* Sample P2 to sample C2 were collected for 24 h on the sampling date, while Sample P1 was collected for only 12 h on the sampling date.

distributions were derived from the number size distributions under the assumption of spherical geometry for normalization of INP concentrations.

2.2. INP measurements

As described by Chen et al. (2021), filters from each MOUDI stage were subjected to ultrasonic extraction in 20 mL of double-distilled water (resistivity of 18.2 MΩ·cm at 25 °C) for 30 min to detach particles from the filter matrix. The resulting particle suspensions were subsequently used for ice nucleation measurements and chemical analyses.

Immersion freezing experiments were conducted by the PeKing University Ice Nucleation Array (PKUINA), a cold-stage-based system (Chen et al., 2018a). Prior to each measurement, the suspensions were vortexed for more than 10 s to ensure homogeneity. 90 aliquots (1 μL each) were then dispensed onto a hydrophobic glass slide mounted on the cold stage. Individual droplets were physically separated using a spacer block and cover slides to prevent interactions associated with the Wegener–Bergeron–Findeisen process. Droplet freezing was monitored by a charge-coupled device during cooling at a controlled rate of 1 °C min^{-1}, with images recorded every 6 s until complete freezing occurred.

The frozen fractions (f_{ice}) is defined as:

$$f_{ice} = \frac{N_{frozen}}{N_t} \tag{1}$$

where N_{frozen} refers to the proportion of droplets that have frozen relative to the total of 90 droplets at a given temperature.

The cumulative number concentration of INP (N_{INP}) per unit volume of sampled air (Vali, 1971) can be determined as:

$$N_{INP}(T) = \frac{-\ln(1 - f_{ice}(T))}{V_{air}} \left(L^{-1} air\right) \tag{2}$$

where f_{ice}(T) corresponds to the fraction of frozen droplets among the 90 droplets at temperatures exceeding T, and V_{air} represents the total air volume sampled per droplet during each sampling period under standard conditions (0 °C, 1013 hPa).

To facilitate comparison of IN activity, particularly for mineral dust particles, the cumulative ice nucleation active site density (n_s) is adopted (Connolly et al., 2009; Niemand et al., 2012), the number of active sites per unit surface area of INPs (Vali et al., 2015) is obtained from the N_{INP} as:

$$n_s(T) = \frac{N_{INP}(T)}{A} \left(m^{-2}\right) \tag{3}$$

where A denotes the particle surface area per unit volume of sampled air, calculated from online particle number–size distribution data assuming spherical particles characterized by aerodynamic diameter at standard temperature and pressure (0 °C, 1013 hPa).

2.3. Chemical analysis

Water-soluble inorganic ions and elemental compositions were analyzed using the same aqueous suspensions prepared for ice nucleation measurements. For ionic analysis (Na^+, Mg^{2+}, K^+, Ca^{2+}, NH_4^+, NO_3^-, SO_4^{2-}, and Cl^-), suspensions were filtered through 0.45 μm polyethersulfone (PES) membrane filters and analyzed by ion chromatography (DIONEX ICS-2000/Integrion). Elemental concentrations were measured using inductively coupled plasma mass spectrometry (ICP-MS), targeting elements including Na, Mg, Al, K, Ca, Ti, Mn, Fe, Zn, As, Ba, and Pb. Elemental concentrations determined by ICP-MS were converted to oxide compositions (e.g., Fe_2O_3, Al_2O_3, and SiO_2) using stoichiometric molecular-weight relationships (Malm et al., 1994; Marconi et al., 2014).

Since ion chromatography cannot detect CO_3^{2-}, some studies estimate the carbonate ion concentration from the ion-balance discrepancy during dust events (i.e., the sum of cation equivalents minus the sum of anion equivalents) (Cao et al., 2005; Huang et al., 2010). The uncertainties of this method include potential charge imbalance from unmeasured ionic species (e.g., organic acids, trace metals) (Noguchi and Hara, 2004), overestimation of carbonate due to cation contributions from metal oxides (Jankowski et al., 2008), and underestimation of actual carbonate content due to incomplete dissolution of calcium carbonate particles (Piazzalunga et al., 2013).

2.4. Metagenomic analysis

To characterize the microbial community associated with dust-influenced aerosols, total suspended particulate (TSP) samples were collected in parallel during dust-affected pollution events using high-volume air samplers (TH-1000C II, Wuhan Tianhong Instruments Co., Ltd., China) with a flow rate of approximately 1 m^3/min. Samples were obtained and stored at −20 °C under sterile conditions. Particulate matter was recovered through centrifugation and resuspension following the enrichment protocol described by Be et al. (2015), after which the concentrates were filtered onto 47 mm PES membranes. The resulting pellets were stored at −80 °C prior to DNA extraction. Genomic DNA was extracted using the MO-BIO PowerSoil DNA Isolation Kit (USA), and DNA quality and concentration were assessed with a NanoDrop ND-1000 spectrophotometer (Maki et al., 2018; Xue et al., 2025). Metagenomic sequencing was performed by Megigene (Guangzhou, China) on the Illumina HiSeq 2000 platform using a paired-end 150 bp strategy, generating approximately 10 Gb of clean data per sample. Low-quality reads, adapter sequences, and reads shorter than 150 bp were removed prior to downstream analysis. Subsequent bioinformatic analyses were conducted using Python based on datasets provided through the Megigene cloud platform (https://cloud.magigene.com/).

3. Results and discussions

3.1. Overview of the pollution/particle concentrations

The detailed sampling information for the seven samples collected from May to October 2025 is presented in Table 1. The total sampling volume and PM_{10} mass concentrations during the sampling period determine the quantity of collected particles and influence the INP concentration. Lanzhou is located along the dust transport pathways of the Taklamakan Desert and the Gobi Desert, making its particulate matter concentration highly susceptible to dust events. In accordance with the definition of dust events established by Chen et al. (2021), a dust event is identified based on a combination of criteria including the PM_{10} concentrations, coarse-mode volume concentrations, aluminum (Al) concentrations, and whether the event is recorded as a large-scale dust weather process by the China Meteorological Administration (CMA). According to this definition, although samples P2 and P5 in this study recorded hourly PM_{10} concentrations exceeding 200 μg·m^{-3} for durations longer than two hours, their sampling periods did not coincide with large-scale dust events documented by the CMA. Consequently, these two samples are not classified as dust events, yet they were still influenced by dust to some extent.

Among the seven samples, two exhibited PM_{10} concentrations below 50 μg·m^{-3} and were thus classified as clean days (Ganor and Foner, 1996). The $PM_{2.5}/PM_{10}$ ratios for these two samples were 0.45 and 0.52, significantly lower than those observed on clean days in humid eastern regions. Consequently, categorizing atmospheric conditions in Lanzhou as “clean” is relative compared to many other areas. Due to the region's proximity to dust sources, dust particles persistently exist in the air even in the absence of dust storms. In this study, the PM_{10} concentrations observed were significantly lower than those reported by Ardon-Dryer and Levin (2014) and Chen et al. (2021) during intense dust events in the eastern Mediterranean (approximately 400–800 μg·m^{-3})

and Beijing (approximately 200–1000 μg·m^{-3}). The $PM_{2.5}/PM_{10}$ ratio ranged from 0.33 to 0.52, markedly higher than the ratios observed in dust events in eastern Mediterranean and Beijing (approximately 0.2), but lower than the results reported by Chen et al. (2024) for anthropogenic dust sampled during summer in Beijing (0.6–0.85). This pattern suggests that the samples in this study represent a mixture of natural dust and anthropogenic pollution. We have compared the 7 samples with long-term meteorological and pollution records to demonstrate that these samples capture the typical variability during the sampling period. As shown in Fig. S1, almost all sampling points lie within the 25th–75th percentile (IQR) or within the 5th–95th percentile range for temperature, RH, wind speed, PM_{10} and the ratio of $PM_{2.5}/PM_{10}$, indicating the samples are representative of typical winter/spring conditions in Lanzhou.

3.2. INP Concentration

Fig. 1(a) shows the total ice-nucleating particle concentration (NINP, sum of size-resolved NINP) across different days as a function of temperature. The temperature-dependent trends of total NINP are consistent, with variations remaining within one order of magnitude over the temperature range of −25 °C to −5 °C. Among them, samples collected on May 16 (P2) and September 15 (P5) were influenced by dust, resulting in elevated INP concentrations. As illustrated in Fig. 1(b), the INP concentrations measured in Lanzhou were compared with results from other studies. The INP concentrations in dust-affected samples (P2 and P5) approached the upper bound of the NINP range derived from precipitation samples compiled by Petters and Wright (2015), yet remained substantially lower than values observed in Beijing during large-scale dust events in East Asia (Chen et al., 2021). INP concentrations in the other samples fell within the NINP range reported by Petters and Wright (2015), were higher than those measured under anthropogenic pollution conditions in Beijing (Chen et al., 2018b), and were comparable to the levels observed for anthropogenic dust in Beijing (Chen et al., 2024). These results indicate that due to the persistent presence of dust particles in the background atmosphere of Lanzhou, INP concentrations are moderately elevated compared to regions dominated primarily by anthropogenic pollution.

Notably, a potential limitation of the MOUDI sampling technique that may affect the interpretation of our coarse-mode INP data is particle bounce. As noted in Section 2.1, particle bounce may influence the interpretation of coarse-mode INP data in several ways. Coarse particles may be under-collected, leading to an underestimation of coarse-mode INP concentrations; *Re*-entrainment of bounced particles into smaller stages may artificially enhance the apparent contribution of fine-mode INPs; The inferred size dependence of INP activity may therefore be biased. These may result in lower contributions of coarse-mode INP in this study to some extent. In this study, the INP concentrations at 5.6 and 10 μm were lower than those at 3.2 μm in some samples.

Compared with previous studies on INP in the semi-arid regions of Northwest China, the mean INP concentration observed in this study (0.88 L^{-1}) is comparable to the order of magnitude (~10^0) reported by Niu et al. (2000) in the Helan Mountain region, slightly higher than the values (~10^{-1}) reported by Chen (1994) in Inner Mongolia. Overall, the value is higher than the concentrations (~10^{-3} to 10^{-1}) reported by Zhao et al. (1965) in Lanzhou but lower than the observations reported by Li and Du (2003) in Lanzhou (5.2 L^{-1} and 11.1 L^{-1}). Both the INP concentration 1.07 L^{-1}(dust) and 0.71 L^{-1}(non-dust) are lower than those reported by Jiang et al. (2016) in Xinjiang (51.8 L^{-1} during dust events and 10.8 L^{-1} during non-dust periods). These discrepancies may be attributed to differences in measurement techniques, variations in atmospheric chemical composition, and variable dust intensities during the research, particularly the influence of dust event frequency and severity.

3.3. The chemical composition and INP concentration

The mass fractions of water-soluble ions in the seven samples are shown in Fig. 2. In the clean samples (C1 and C2), the chemical composition of submicron particles was dominated by sulfate and ammonium, with a relatively low contribution of calcium. In the polluted samples, calcium accounted for a high proportion (> 50%) in the submicron particles, while the contribution of secondary inorganic salts was relatively low (~ 20%). The fraction of calcium ions was even higher in the supermicron particles (3.2 μm). In the clean samples, the proportion of calcium ions in the supermicron particles also increased substantially. (See Figs. 3 and 4.)

Asian dust inherently contains abundant carbonate minerals in its surface soils and rocks, particularly calcite ($CaCO_3$). The high proportion of calcium ions and the relatively low proportions of sulfate and nitrate ions suggest that the detected water-soluble calcium ions likely originate mainly from the slight dissolution of carbonate minerals themselves. Since ion chromatography cannot detect CO_3^{2-}, some studies estimate the carbonate ion concentration from the ion-balance discrepancy during dust events (i.e., the sum of cation equivalents minus the sum of anion equivalents) (Cao et al., 2005; Huang et al., 2010). In this study, ion-balance calculations revealed an anion deficit in each sample during the observation period. The strong correlation (R^2 = 0.95–0.99)

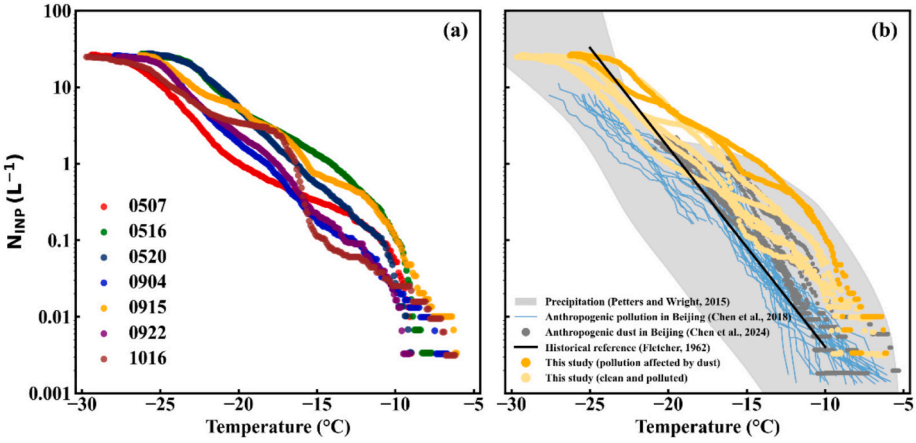

Fig. 1. (a) N_{INP} in this study. (b) N_{INP} as derived from precipitation samples (Petters and Wright, 2015) (grey area), anthropogenic pollution in Beijing (Chen et al., 2018b) (blue line), anthropogenic dust in Beijing (Chen et al., 2024) (grey scatter plot) and a parameterization based on Fletcher (1962) (black line), together with our results (Dark yellow scatter points indicate pollution affected by dust, and light yellow scatter points indicate both clean and polluted episodes.). (For interpretation of the references to colour in this figure legend, the reader is referred to the web version of this article.)

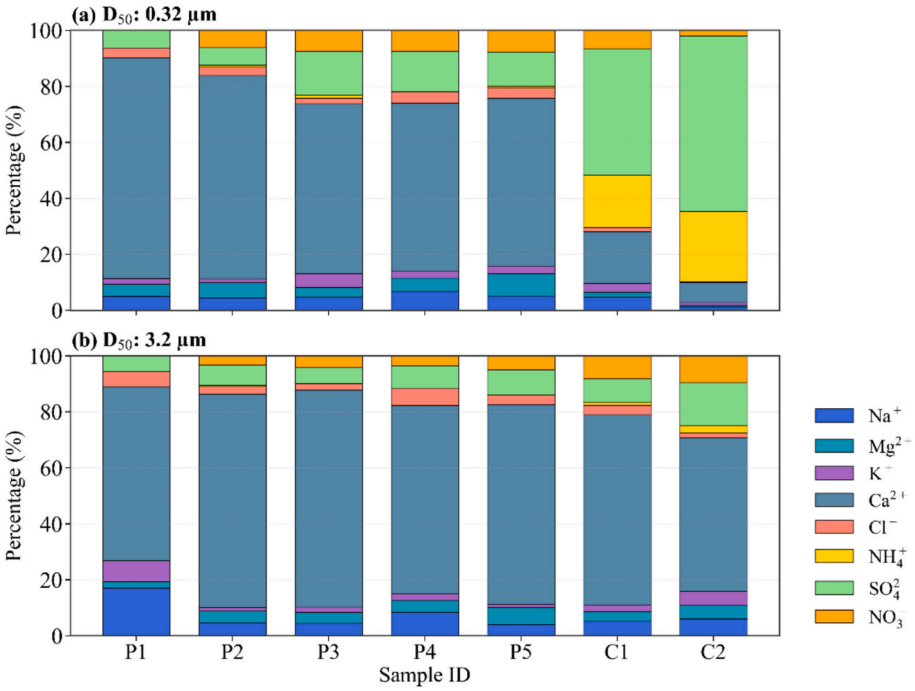

Fig. 2. The fractions of water-soluble ions with different sizes.

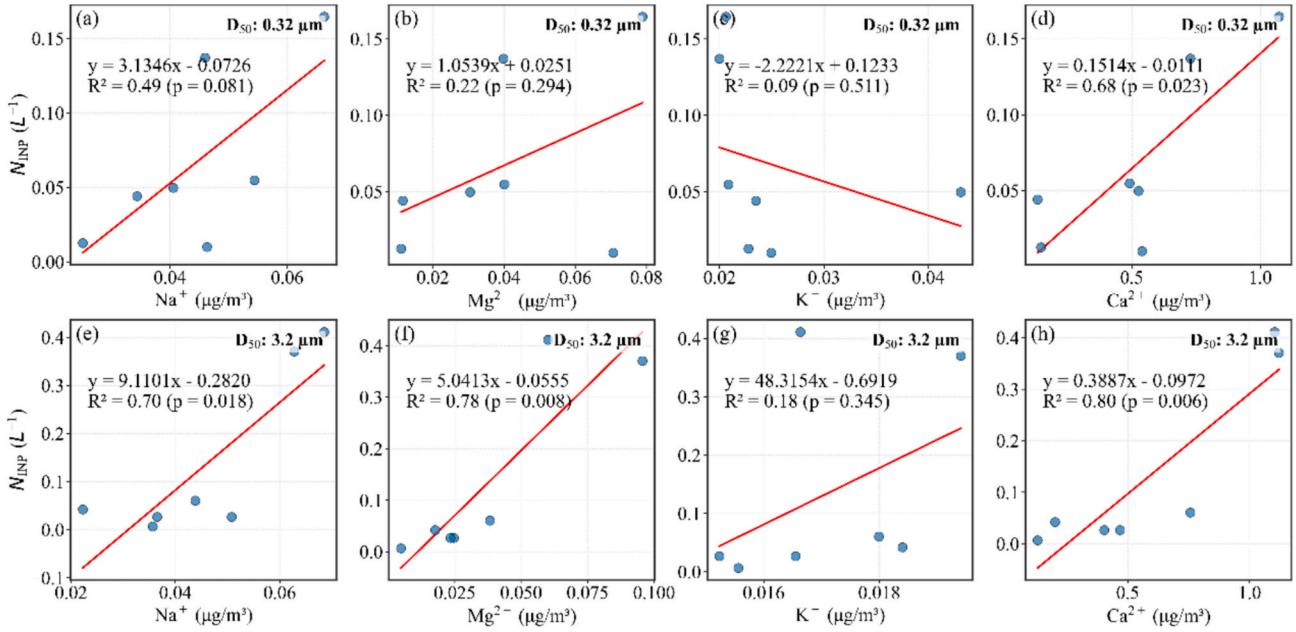

Fig. 3. The correlations between N_{INP} and the mass concentrations of metal ions (sodium ion (Na^+), magnesium ions (Mg^{2+}), potassium ion (K^+) and calcium ions (Ca^{2+}) in D_{50} = 0.32 μm and D_{50} = 3.2 μm particles.

between measured calcium ions and estimated carbonate ions across all particle-size fractions indicates that the missing anions are likely carbonate species (Zhu and Yang, 2010).

As shown in Fig. 2 and supported by the above analysis, the high calcium ions originate primarily from the slight dissolution of carbonate minerals themselves, along with a minor contribution from the physical dissolution of soluble salts (e.g., gypsum, $CaSO_4{\cdot}2H_2O$) present in the source-region soils (Wang et al., 2014; Wu et al., 2020). This finding suggests that dust particles undergo limited aging upon transport to Lanzhou. Specifically, during the transport of dust to the relatively dry semi-arid region, low relative humidity suppresses the liquid-phase heterogeneous reactions between gaseous pollutants (SO_2, NOx) and dust surfaces (e.g., $CaCO_3$). Consequently, the formation of secondary products such as calcium nitrate, ammonium sulfate, and ammonium nitrate are inhibited. In the contrast, dust transported to the humid eastern regions often undergoes sufficient aging processes, generating substantial amounts of secondary inorganic aerosols (Wu et al., 2020).

Certain metal ions exhibited correlations with INP concentrations (See Fig. 3). For instance, at −16 °C, INP concentrations showed relatively strong correlations with calcium ions in both the 0.32 μm and 3.2 μm (R^2 = 0.68–0.80, $P < 0.05$). Sodium and magnesium also demonstrated good correlations with INP concentrations in 3.2 μm (R^2 =

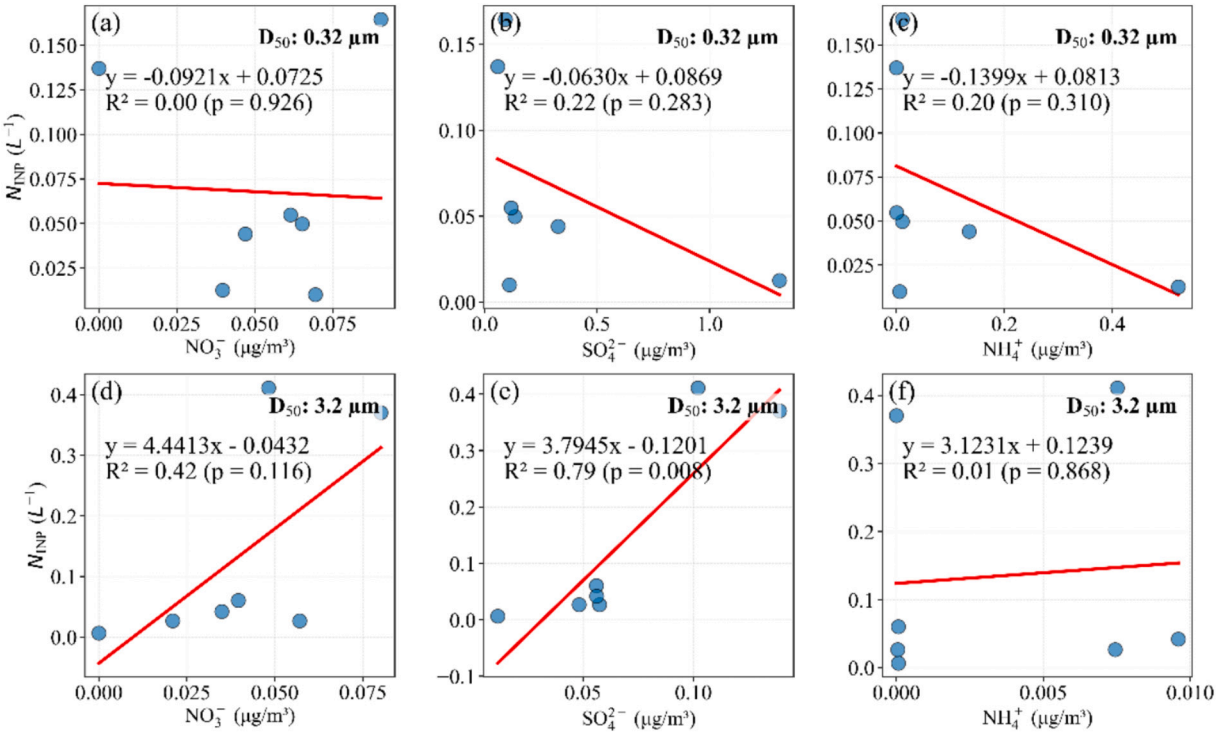

Fig. 4. The correlations between N_{INP} and the mass concentrations of nitrate ion (NO_3^-), sulfate ions (SO_4^{2-}) and ammonium ion (NH_4^+) in D_{50} = 0.32 μm and D_{50} = 3.2 μm particles.

0.70–0.78). A significant raw correlation was observed between Ca^{2+} and INP concentrations in the 3.2 μm fraction (r = 0.80, $p < 0.05$). However, after controlling for total particle surface area, the partial correlation was not statistically significant (partial r = 0.73, $p > 0.05$, n = 7), and n_s showed no correlation with Ca^{2+} (r = 0.04, $p > 0.05$). These results indicate that the observed association between Ca^{2+} and INP concentrations is primarily driven by surface area effects, rather than a specific chemical enhancement of ice nucleation activity by Ca^{2+}-rich particles. Thus, surface area appears to be the dominant factor controlling INP concentrations in the large particle size. Time series analysis (Fig. S2) also shows a certain degree of synchronous variation between INP concentration and dust tracers (calcium ions), as well as with total surface area. For example, samples P2, P3, and P5 exhibited higher INP concentrations, which corresponded to larger surface areas and higher proportions of calcium ions. Meanwhile, samples C1 and C2 showed lower INP concentrations, along with lower surface areas and lower calcium ion concentrations.

3.4. Parameterizations of size-resolved ice-nucleation-active site densities

New $n_s(T)$ parameterizations for size-resolved ice-nucleation-active-site densities of dust particles are calculated by an exponential function:

$$n_s(T) = \exp(a \cdot T + b)\left(m^{-2}\right) \quad (4)$$

In this equation, T represents temperature in degrees Celsius, with coefficients a and b provided in Table 2. The parameterization considered four particle sizes measured in this study: D_{50} = 5.6, 3.2, 1.8, and 1.0 μm. Size-resolved freezing efficiencies for dust particles are shown in Fig. 5a, and the corresponding fitting coefficients are listed in Table 2. A clear dependence on particle size was observed: the fitted curve for 5.6 μm exhibited the highest freezing efficiency. In contrast, the curves for D_{50} = 3.2 μm, 1.8 μm, and 1.0 μm nearly overlapped. These were therefore averaged to generate a composite curve representing the 1.0–3.2 μm size range, as presented in Fig. 5b.

Table 2
Parameterization coefficients for different size classes based on this study.

Fit line	Coefficients	R^2	Valid T range (°C)
5.6 μm fit line	a = −0.359, b = 4.026	0.65	−30 to −5
3.2 μm fit line	a = −0.313, b = 3.305	0.71	−30 to −5
1.8 μm fit line	a = −0.324, b = 2.427	0.69	−30 to −5
1.0 μm fit line	a = −0.311, b = 3.328	0.68	−30 to −5

We compared the size-resolved parameterization from this study with previous results derived from desert dust and single mineral dust components. Overall, the ice nucleating active site density (n_s) obtained in this study aligns reasonably well with the parameterization for quartz (Harrison et al., 2019), and shows consistency with the supermicron results of Reicher et al. (2019) at temperatures above −15 °C. However, it remains 2–3 orders of magnitude lower than the values reported for potassium feldspar (Atkinson et al., 2013), large-scale East Asian dust events (Chen et al., 2021), and dust samples (Niemand et al., 2012).

The variation of n_s with particle size in this study is similar to the results observed by Chen et al. (2021) during large-scale East Asian dust events in Beijing. However, the values of n_s in our study are 2–3 orders of magnitude lower. The discrepancy may be attributed to the difference in dust input intensity between the two studies. In the study by Chen et al., the PM_{10} concentration was significantly higher, with a peak value reaching 1145 μg m^{-3}, whereas in the present study, although dust input was observed, both its intensity was substantially lower than those reported by Chen et al. Additionally, Chen et al. (2021) demonstrated that proteinaceous biological materials, quantified as heat-sensitive INPs, substantially influence the ice nucleation properties of Asian airborne mineral dust at elevated temperatures. In this study, although the contribution of heat-sensitive INPs was not directly quantified, metagenomic analyses were performed on two dust-influenced samples. The results showed that the relative abundance of *Pseudomonas* in these samples was comparable to that reported in previous studies conducted during dust events, where *Pseudomonas* is consistently detected as a minor but recurrent bacterial taxon (Lim et al., 2011; Maki et al., 2018; Xue et al., 2025). Although the relative contribution of *Pseudomonas* at

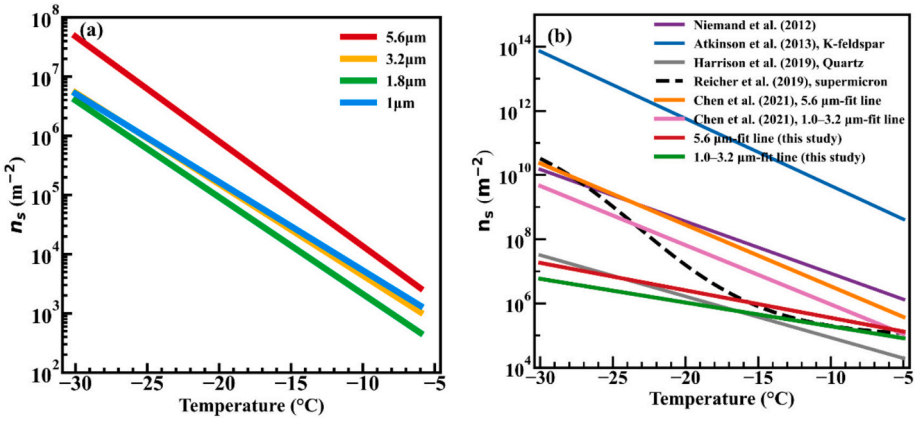

Fig. 5. Parameterizations of ice-nucleation-active-site densities for different size classes. (a) Parameterizations developed from this study. (b) Comparison between the parameterizations derived from this study and those for desert dust (Niemand et al., 2012; Reicher et al., 2019; Chen et al., 2021) and single-mineral dust components (Atkinson et al., 2013; Harrison et al., 2019).

the phylum level to the total bacterial community was similar to that reported in previous dust-related studies (Maki et al., 2018), the total bacterial abundance measured in this study was 10^1 culture-equivalent bacterial abundance (CFU m^{-3} air), markedly lower than values reported during dust events, which was approximately 10^1–10^2 CFU m^{-3} in Australian dust storms (Lim et al., 2011) and 10^4–10^7 cells m^{-3} during Asian dust (Kosa) events (Maki et al., 2014). This discrepancy suggests that although potentially ice-nucleation-active bacteria were present during the sampling period of this study, their contribution to the INPs was likely limited due to their low abundance, which also partly explains the relatively low n_s observed in this study compared to strong dust events.

The n_s in this study are roughly three orders of magnitude lower than those reported for K-feldspar (Atkinson et al., 2013). Potassium (K) can originate from both natural origins (e.g., dust particles such as feldspar) and human activities (e.g., biomass burning and coal combustion; Yu et al., 2018). Although this study could not directly quantify the K-feldspar content, the mass concentrations of Ca and K showed no significant correlation in either submicron or supermicron particles. This may indicate that K was more likely primarily derived from combustion processes rather than from dust particles (Fig. S7). This contrasts with findings in anthropogenic dust in Beijing (Chen et al., 2024). Therefore, we further infer that the content of potassium feldspar transported with dust during the observation period of this study was likely low, which partly explains why the ice-nucleating activity of particles remained relatively low despite the presence of dust input. The mineral composition results indicate that both submicron and supermicron particles are predominantly composed of calcium oxide, with quartz also constituting a significant component (Fig. S4).

In summary, the relatively low n_s in this study are mainly associated with several factors during the sampling period, including weak dust intensity, low content of biological INPs, and a limited presence of mineral components with high ice-nucleating activity (K-feldspar). Our results represent typical conditions in Lanzhou. Long-term historical pollution observations indicate that the probability of intense dust events occurring in Lanzhou during recent years is low, and the more frequently occurring pollution process is the mixture of dust and anthropogenic pollution. The low content of biological INPs and the limited presence of K-feldspar are likely attributable to the regional soil composition (characterized by loess with relatively low K-feldspar content compared to desert sources) and the significant dilution effect of anthropogenic pollution typical of this semi-arid urban environment. The parameterization scheme developed here is applicable to mixed scenarios involving both dust and anthropogenic pollution in semi-arid regions.

4. Conclusion

In this study, we report the INP number concentration, surface active-site density (n_s), and chemical compositions (water-soluble ions and metal elements) of urban particles in different size classes in Lanzhou, a typical semi-arid city near the dust source regions. The $PM_{2.5}/PM_{10}$ ratio ranged from 0.33 to 0.52, markedly higher than the ratios observed in dust events in eastern Mediterranean and Beijing (approximately 0.2), but lower than the results reported by Chen et al. (2024) for anthropogenic dust sampled during summer in Beijing (0.6–0.85). This pattern suggests that the samples in this study represent a mixture of natural dust and anthropogenic pollution. The total concentration of immersion-mode INPs measured in this study varied between 0.05 and 19.60 L^{-1} across a temperature interval of −25 °C to −10 °C. Due to the persistent presence of dust particles in the background atmosphere of Lanzhou, INP concentrations are moderately elevated compared to regions dominated by anthropogenic pollution.

Chemical composition analysis revealed that during pollution episodes, the proportion of calcium was high even in submicron particles, while the contribution of secondary inorganic aerosols was low. This finding suggests that the aging degree of dust in Lanzhou is limited due to the low humidity conditions. Specifically, during the transport of dust to the relatively dry semi-arid region, low relative humidity suppresses the liquid-phase heterogeneous reactions between gaseous pollutants (SO_2, NOx) and dust surfaces (e.g., $CaCO_3$). A significant raw correlation was observed between Ca^{2+} and INP concentrations in the 3.2 μm fraction. However, after controlling for total particle surface area, the partial correlation was not statistically significant and ns showed no correlation with Ca^{2+}. These results indicate that the observed association between Ca^{2+} and INP concentrations is primarily driven by surface area effects, rather than a specific chemical enhancement of ice nucleation activity by Ca^{2+}-rich particles. Thus, surface area appears to be the dominant factor controlling INP concentrations in the large particle size.

We propose a new parameterization scheme for INP activity that is based on size-resolved nucleation properties (n_s) and is applicable to mixed conditions of dust and anthropogenic pollution. The relatively low n_s values in this study are mainly associated with several factors during the sampling period, including weak dust intensity, low content of biological INPs, and a limited presence of mineral components with high ice-nucleating activity (K-feldspar). The parameterization scheme developed here is applicable to mixed scenarios involving both dust and anthropogenic pollution in semi-arid regions.

CRediT authorship contribution statement

Jiayun Li: Writing – original draft, Visualization, Validation, Software, Methodology, Investigation, Formal analysis, Data curation, Conceptualization. **Dantong Chen:** Visualization, Validation, Software, Methodology, Formal analysis, Data curation. **Yiyang Gao:** Software, Methodology, Formal analysis, Data curation. **Zhijun Wu:** Writing – review & editing, Supervision, Resources. **Jiawei Yang:** Supervision, Resources. **Pengfei Tian:** Supervision, Resources. **Yuan Wang:** Supervision, Resources. **Zirui Liu:** Supervision, Resources. **Lei Zhang:** Supervision, Resources. **Zhongwei Huang:** Writing – review & editing, Supervision.

Declaration of competing interest

The authors declare that they have no known competing financial interests or personal relationships that could have appeared to influence the work reported in this paper.

Acknowledgements

This research was supported by the National Natural Science Foundation of China (42205096) and the National Key Research and Development Program of China (2023YFC3708202). The authors gratefully acknowledge Ji Zhao for providing the particle size spectrometer observational data.

Appendix A. Supplementary data

Supplementary data to this article can be found online at https://doi.org/10.1016/j.atmosres.2026.109112.

Data availability

Data will be made available on request.

References

Ardon-Dryer, K., Levin, Z., 2014. Ground-based measurements of immersion freezing in the eastern Mediterranean. Atmos. Chem. Phys. 14, 5217–5231. https://doi.org/10.5194/acp-14-5217-2014.

Atkinson, J.D., Murray, B.J., Woodhouse, M.T., Whale, T.F., Baustian, K.J., Carslaw, K.S., Dobbie, S., O'Sullivan, D., Malkin, T.L., 2013. The importance of feldspar for ice nucleation by mineral dust in mixed-phase clouds. Nature 498, 355–358. https://doi.org/10.1038/nature12278.

Be, N.A., Thissen, J.B., Fofanov, V.Y., Allen, J.E., Rojas, M., Golovko, G., Fofanov, Y., Koshisky, H., Jaing, C.J., 2015. Metagenomic analysis of the airborne environment in urban spaces. Environ. Microbiol. 69, 346–355. https://doi.org/10.1007/s00248-014-0517-z.

Cao, J.J., Lee, S.C., Zhang, X.Y., Chow, J.C., An, Z.S., Ho, K.F., Watson, J.G., Fung, K., Wang, Y.Q., Shen, Z.X., 2005. Characterization of airborne carbonate over a site near Asian dust source regions during spring 2002 and its climatic and environmental significance. J. Geophys. Res. Atmos. 110, 1–8. https://doi.org/10.1029/2004JD005244.

Chen, J.R., 1994. The observation results and its features of the concentration of atmospheric ice nucleus. Sci. Meteorol. Sin. 02, 155–160 (in Chinese).

Chen, J., Pei, X.Y., Wang, H., Chen, J.C., Zhu, Y.S., Tang, M.J., Wu, Z.J., 2018a. Development, characterization, and validation of a cold stage-based ice nucleation array (PKU-INA). Atmosphere 9, 13. https://doi.org/10.3390/atmos9090357.

Chen, J., Wu, Z.J., Augustin-Bauditz, S., Grawe, S., Hartmann, M., Pei, X.Y., Liu, Z.R., Ji, D.S., Wex, H., 2018b. Ice-nucleating particle concentrations unaffected by urban air pollution in Beijing, China. Atmos. Chem. Phys. 18, 3523–3539. https://doi.org/10.5194/acp-18-3523-2018.

Chen, J.C., Wu, Z.J., Chen, J., Reicher, N., Fang, X., Rudich, Y., Hu, M., 2021. Size-resolved atmospheric ice-nucleating particles during East Asian dust events. Atmos. Chem. Phys. 21, 3491–3506. https://doi.org/10.5194/acp-21-3491-2021.

Chen, J., Wu, Z.J., Gong, X.D., Qiu, Y.T., Chen, S.Y., Zeng, L.M., Hu, M., 2024. Anthropogenic dust as a significant source of ice-nucleating particles in the urban environment. Earths Future 12, e2023EF003738. https://doi.org/10.1029/2023EF003738.

Connolly, P.J., Möhler, O., Field, P.R., Saathoff, H., Burgess, R., Choularton, T., Gallagher, M., 2009. Studies of heterogeneous freezing by three different desert dust samples. Atmos. Chem. Phys. 9, 2805–2824. https://doi.org/10.5194/acp-9-2805-2009.

DeMott, P.J., Prenni, A.J., Liu, X., Kreidenweis, S.M., Petters, M.D., Twohy, C.H., Richardson, M.S., Eidhammer, T., Rogers, D.C., 2010. Predicting global atmospheric ice nuclei distributions and their impacts on climate. Proc. Natl. Acad. Sci. 107, 11217–11222. https://doi.org/10.1073/pnas.0910818107.

Fan, J., Leung, L.R., Rosenfeld, D., DeMott, P.J., 2017. Effects of cloud condensation nuclei and ice nucleating particles on precipitation processes and supercooled liquid in mixed-phase orographic clouds. Atmos. Chem. Phys. 17, 1017–1035. https://doi.org/10.5194/acp-17-1017-2017.

Fletcher, N.H., 1962. The Physics of Rainclouds. Cambridge University Press, Cambridge.

Ganor, E., Foner, H., 1996. The mineralogical and chemical properties and the behavior of the aeolian Saharan dust over Israel. Environ. Sci. Technol. Lib. 11. https://doi.org/10.1007/978-94-017-3354-0_15.

Ge, Z.M., Zhou, C.K., 1986. The observations of atmospheric ice nuclei in Lanzhou. Plateau Meteorol. 5, 167–171 (in Chinese).

Gibbons, M., Min, Q., Fan, J., 2018. Investigating the impacts of Saharan dust on tropical deep convection using spectral bin microphysics. Atmos. Chem. Phys. 18, 12161–12184. https://doi.org/10.5194/acp-18-12161-2018.

Harrison, A.D., Lever, K., Sanchez-Marroquin, A., Holden, M.A., Whale, T.F., Tarn, M.D., McQuaid, J.B., Murray, B.J., 2019. The ice-nucleating ability of quartz immersed in water and its atmospheric importance compared to K-feldspar. Atmos. Chem. Phys. 19, 11343–11361. https://doi.org/10.5194/acp-19-11343-2019.

Hawker, R.E., Miltenberger, A.K., Wilkinson, J.M., Hill, A.A., Shipway, B.J., Cui, Z., Cotton, R.J., Carslaw, K.S., Field, P.R., Murray, B.J., 2021. The temperature dependence of ice-nucleating particle concentrations affects the radiative properties of tropical convective cloud systems. Atmos. Chem. Phys. 21, 5439–5461. https://doi.org/10.5194/acp-21-5439-2021.

Hoose, C., Möhler, O., 2012. Heterogeneous ice nucleation on atmospheric aerosols: a review of results from laboratory experiments. Atmos. Chem. Phys. 12, 9817–9854. https://doi.org/10.5194/acp-12-9817-2012.

Huang, K., Zhuang, G., Li, J., Wang, Q., Sun, Y., Lin, Y., Fu, J.S., 2010. Mixing of Asian dust with pollution aerosol and the transformation of aerosol components during the dust storm over China in spring 2007. J. Geophys. Res. Atmos. 115, 1–13. https://doi.org/10.1029/2009JD013145.

Jankowski, N., Schmidl, C., Marr, I.L., Bauer, H., Puxbaum, H., 2008. Comparison of methods for the quantification of carbonate carbon in atmospheric PM10 aerosol samples. Atmos. Environ. 42, 8055–8064. https://doi.org/10.1016/j.atmosenv.2008.06.012.

Jiang, H., Yin, Y., Wang, X., Gao, R., Yuan, L., Chen, K., Shan, Y., 2016. The measurement and parameterization of ice nucleating particles in different backgrounds of China. Atmos. Res. 181, 72–80. https://doi.org/10.1016/j.atmosres.2016.06.013.

Kawai, K., Matsui, H., Tobo, Y., 2021. High potential of Asian dust to act as ice nucleating particles in mixed-phase clouds simulated with a global aerosol-climate model. J. Geophys. Res. Atmos. 126. https://doi.org/10.1029/2020jd034263.

Li, Y., Du, B., 2003. Measurement and analysis of concentration of atmospheric ice nuclei in Tianshan mountain area. Trans. Atmos. Sci. 26, 364–370. https://doi.org/10.3969/j.issn.1674-7097.2003.03.010 (in Chinese).

Lim, N., Munday, C.I., Allison, G.E., O'Loingsigh, T., Deckker, P.D., Tapper, N.J., 2011. Microbiological and meteorological analysis of two Australian dust storms in April 2009. Sci. Total Environ. 412–413, 223–231. https://doi.org/10.1016/j.scitotenv.2011.10.030.

Maki, T., Puspitasari, F., Hara, K., Yamada, M., Kobayashi, K., Hasegawa, H., Iwasaka,Y. 2014. Variations in the structure of airborne bacterial communities in a downwind area during an Asian dust (Kosa) event. Sci. Total Environ. 488–489, 75–84. doi: https://doi.org/10.1016/j.scitotenv.2014.04.044.

Maki, T., Furumoto, S., Asahi, Y., Lee, K.C., Watanabe, K., Aoki, K., Murakami, M., Tajiri, T., Hasegawa, H., Mashio, A., Iwasaka, Y., 2018. Long-range-transported bioaerosols captured in snow cover on Mount Tateyama, Japan: impacts of Asian-dust events on airborne bacterial dynamics relating to ice-nucleation activities. Atmos. Chem. Phys. 18, 8155–8171. https://doi.org/10.5194/acp-18-8155-2018.

Maki, T., Lee, K.C., Kawai, K., Onishi, K., Hong, C.S., Kurosaki, Y., Shinoda, M., Kai, K., Iwasaka, Y., Archer, S.D.J., Lacap-Bugler, D.C., Hasegawa, H., Pointing, S.B., 2019. Aeolian dispersal of bacteria associated with desert dust and anthropogenic particles over continental and oceanic surfaces. J. Geophys. Res. Atmos. 124, 5579–5588. https://doi.org/10.1029/2018jd029597.

Malm, W.C., Sisler, J.F., Huffman, D., Eldred, R.A., Cahill, T.A., 1994. Spatial and seasonal trends in particle concentration and optical extinction in the United States. J. Geophys. Res. Atmos. 99, 1347–1370. https://doi.org/10.1029/93JD02916.

Marconi, M., Sferlazzo, D.M., Becagli, S., Bommarito, C., Calzolai, G., Chiari, M., di Sarra, A., Ghedini, C., Gómez-Amo, J.L., Lucarelli, F., Meloni, D., Monteleone, F., Nava, S., Pace, G., Piacentino, S., Rugi, F., Severi, M., Traversi, R., Udisti, R., 2014. Saharan dust aerosol over the central Mediterranean Sea: PM10 chemical composition and concentration versus optical columnar measurements. Atmos. Chem. Phys. 14, 2039–2054. https://doi.org/10.5194/acp-14-2039-2014.

Marple, V.A., Rubow, K.L., Behm, S.M., 1991. A microorifice uniform deposit impactor (MOUDI): description, calibration, and use. Aerosol Sci. Tech. 14, 434–446. https://doi.org/10.1080/02786829108959504.

Mehta, M., Singh, N., Anshumali., 2018. Global trends of columnar and vertically distributed properties of aerosols with emphasis on dust, polluted dust and smoke - inferences from 10-year long CALIOP observations. Remote Sens. Environ. 208, 120–132. https://doi.org/10.1016/j.rse.2018.02.017.

Mülmenstädt, J., Sourdeval, O., Delanoë, J., Quaas, J., 2015. Frequency of occurrence of rain from liquid-, mixed-, and ice-phase clouds derived from A-Train satellite retrievals. Geophys. Res. Lett. 42, 6502–6509. https://doi.org/10.1002/2015GL064604.

Niemand, M., Möhler, O., Vogel, B., Vogel, H., Hoose, C., Connolly, P., Klein, H., Bingemer, H., DeMott, P., Skrotzki, J., Leisner, T., 2012. A particle-surface-area-

based parameterization of immersion freezing on desert dust particles. J. Atmos. Sci. 69, 3077–3092. https://doi.org/10.1175/jas-d-11-0249.1.
Niu, S., An, X., Chen, Y., Huang, S., 2000. Measurements and Analysis of Concentrations of Atmospheric Ice Nuclei in the Helanshan Area. Trans. Atmos. Sci. 23, 294–298. https://doi.org/10.13878/j.cnki.dqkxxb.2000.02.021 (in Chinese).
Noguchi, I., Hara, H., 2004. Ionic imbalance due to hydrogen carbonate from Asian dust. Atmos. Environ. 38, 6969–6976. https://doi.org/10.1016/j.atmosenv.2004.03.077.
Petters, M.D., Wright, T.P., 2015. Revisiting ice nucleation from precipitation samples. Geophys. Res. Lett. 42, 8758–8766. https://doi.org/10.1002/2015GL065733.
Piazzalunga, A., Bernardoni, V., Fermo, P., Vecchi, R., 2013. Optimisation of analytical procedures for the quantification of ionic and carbonaceous fractions in the atmospheric aerosol and applications to ambient samples. Anal. Bioanal. Chem. 40, 1123–1132. https://doi.org/10.1007/s00216-012-6433-5.
Reicher, N., Budke, C., Eickhoff, L., Raveh-Rubin, S., Kaplan-Ashiri, I., Koop, T., Rudich, Y., 2019. Size-dependent ice nucleation by airborne particles during dust events in the eastern Mediterranean. Atmos. Chem. Phys. 19, 11143–11158. https://doi.org/10.5194/acp-19-11143-2019.
Tan, I., Storelymo, T., Zelinka, M.D., 2016. Observational constraints on mixed-phase clouds imply higher climate sensitivity. Science 352, 224–227. https://doi.org/10.1126/science.aad5300.
Vali, G., 1971. Quantitative evaluation of experimental results an the heterogeneous freezing nucleation of supercooled liquids. J. Atmos. Sci. 28, 402–409. https://doi.org/10.1175/1520-0469(1971)028<0402:QEOERA>2.0.CO;2.
Vali, G., DeMott, P.J., Möhler, O., Whale, T.F., 2015. Technical note: a proposal for ice nucleation terminology. Atmos. Chem. Phys. 15, 10263–10270. https://doi.org/10.5194/acp-15-10263-2015.
Vergara-Temprado, J., Miltenberger, A.K., Furtado, K., Grosvenor, D.P., Shipway, B.J., Hill, A.A., Wilkinson, J.M., Field, P.R., Murray, B.J., Carslaw, K.S., 2018. Strong control of Southern Ocean cloud reflectivity by ice-nucleating particles. Proc. Natl. Acad. Sci. 115, 2687–2692. https://doi.org/10.1073/pnas.1721627115.
Wang, G.H., Cheng, C.L., Huang, Y., Tao, J., Ren, Y.Q., Wu, F., Meng, J.J., Li, J.J., Cheng, Y.T., Cao, J.J., Liu, S.X., Zhang, T., Zhang, R., Chen, Y.B., 2014. Evolution of aerosol chemistry in Xi'an, inland China, during the dust storm period of 2013 – Part 1: Sources, chemical forms and formation mechanisms of nitrate and sulfate. Atmos. Chem. Phys. 14, 11571–11585. https://doi.org/10.5194/acp-14-11571-2014.
Wang, Y., Jia, C., Tao, J., Zhang, L., Liang, X., Ma, J., Gao, H., Huang, T., Zhang, K., 2016. Chemical characterization and source apportionment of PM2.5 in a semi-arid and petrochemical-industrialized city, Northwest China. Sci. Total Environ. 573, 1031–1040. https://doi.org/10.1016/j.scitotenv.2016.08.179.
Wu, C., Zhang, S., Wang, G., Lv, S., Li, D., Liu, L., Li, J., Liu, S., Du, W., Meng, J., Qiao, L., Zhou, M., Huang, C., Wang, H., 2020. Efficient heterogeneous formation of ammonium nitrate on the saline mineral particle surface in the atmosphere of East Asia during dust storm periods. Environ. Sci. Technol. 54, 15622–15630. https://doi.org/10.1021/acs.est.0c04544.
Xue, F., Huang, Z., Huo, X., Dong, Q., Li, Z., Gu, Q., 2025. The diversity of airborne bacteria over the Tibet Plateau decreased by Taklimakan dust. Geophys. Res. Lett. 52, e2024GL111830. https://doi.org/10.1029/2024GL111830.
You, L.G., 1976. Ice nuclei in the atmosphere. Meteorol. Mon. 2, 29–32. https://doi.org/10.7519/j.issn.1000-0526.1976.11.018 (in Chinese).
Yu, J., Yan, C., Liu, Y., Li, X., Zhou, T., Zheng, M., 2018. Potassium: a tracer for biomass burning in Beijing? Aerosol Air Qual. Res. 18, 2447–2459. https://doi.org/10.4209/aaqr.2017.11.0536.
Zhao, J.P., Zhang, M., Wang, Y.X., Chen, Z.H., Lai, D.J., 1965. Analysis of atmospheric ice nuclei observations in northern China. Acta. Meteor. Sin. 35, 416–422. https://doi.org/10.11676/qxxb1965.048.
Zhao, B., Wang, Y., Gu, Y., Liou, K.-N., Jiang, J.H., Fan, J., Liu, X., Huang, L., Yung, Y.L., 2019. Ice nucleation by aerosols from anthropogenic pollution. Nat. Geosci. 12, 602–607. https://doi.org/10.1038/s41561-019-0389-4.
Zhu, B., Yang, X., 2010. The origin and distribution of soluble salts in the sand seas of Northern China. Geomorphology 123, 232–242. https://doi.org/10.1016/j.geomorph.2010.07.001.